Influences of screw dislocations on electroluminescence of AlGaN/AlN-based UVC LEDs

Dong Liu 🆔, Sang June Cho 🆔, Huilong Zhang 🆔, Corey R. Carlos, Akhil R. K. Kalapala, Jeongpil Park 🆔, Jisoo Kim, Rafael Dalmau 🆔, Jiarui Gong, Baxter Moody, Xudong Wang, John D. Albrecht, Weidong Zhou, and Zhenqiang Ma 🆔
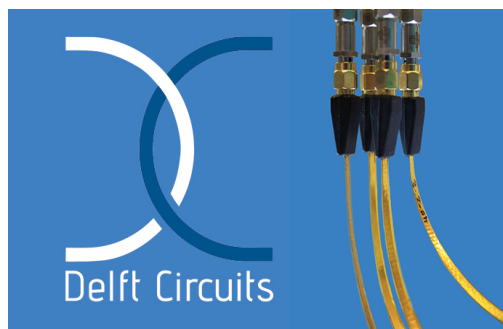
Influences of screw dislocations on electroluminescence of AlGaN/AlN-based UVC LEDs

View Online   Export Citation   CrossMark

Dong Liu,[1,a] **Sang June Cho,**[1,a] **Huilong Zhang,**[1] **Corey R. Carlos,**[2] **Akhil R. K. Kalapala,**[3]
Jeongpil Park,[1] **Jisoo Kim,**[1] **Rafael Dalmau,**[4] **Jiarui Gong,**[1] **Baxter Moody,**[4] **Xudong Wang,**[2]
John D. Albrecht,[5,b] **Weidong Zhou,**[3,b] **and Zhenqiang Ma**[1,b]

AFFILIATIONS

[1] Department of Electrical and Computer Engineering, University of Wisconsin-Madison, Madison, Wisconsin 53706, USA

[2] Department of Material Science Engineering, University of Wisconsin-Madison, Madison, Wisconsin 53706, USA

[3] Department of Electrical Engineering, University of Texas at Arlington, 500 South Cooper Street, Arlington, Texas 76019, USA

[4] HexaTech, Inc., 991 Aviation Parkway, Suite 800, Morrisville, North Carolina 27560, USA

[5] Department of Electrical and Computer Engineering, Michigan State University, 428 S. Shaw Lane, East Lansing, Michigan 48824, USA

[a] **Contributions:** Dong Liu and Sang June Cho contributed equally to this work.
[b] **Authors to whom correspondence should be addressed. Emails:** mazq@engr.wisc.edu or wzhou@uta.edu or jalbrech@egr.msu.edu

ABSTRACT

We investigated two types of threading dislocations in high Al-composition $Al_{0.55}Ga_{0.45}N$/AlN multiple quantum well (MQW) structures grown on AlN substrate for electrically injected deep ultraviolet light-emitting diodes (LEDs). The surface morphology and defects electrical characteristics of the MQW LED structures were examined via conductive atomic force microscopy (CAFM). We found that the disparity between photoluminescence (PL) and electroluminescence (EL) spectra in terms of light emission output and wavelength shift are attributed to the existence of the surface hillocks, especially to the ones that have open-core dislocations. The open-core dislocations form current leakage paths through their defect states and the composition inhomogeneity (*i.e.*, Ga rich) at the dislocation sites are responsible for the light emission at longer wavelengths.

Deep ultraviolet (DUV) AlGaN-based light-emitting diodes (LEDs) have been intensively studied in recent years due to its wide range of applications in photolithography,[1] biological agent sensing,[2] water sterilization[3] and optical data storage.[4] As DUV LEDs are explored toward shorter wavelengths, the Al composition in $Al_xGa_{1-x}N$ during the epi-layer growth is required to increase accordingly to obtain a wider bandgap. However, the efficiency of UVC LEDs are significantly inferior compared to their UVA and UVB counterparts due to several technical challenges, including threading dislocation density (TDD), low hole concentration of p type AlGaN with high Al content, and reduced light extraction efficiency.[5,6] It has been demonstrated that the structural properties of AlGaN layers, especially TDD and surface morphology, severely limit the efficiency of the LEDs.[7–9] The dislocations are known to be detrimental to the performance of DUV LEDs, as they may lead to non-radiative recombination centers and thus current leaky paths across the quantum wells layers.[10,11] Furthermore, the dislocations manifest as protruding hillocks on the top surface of finished epitaxial structures.

Another critical challenge in realizing high-performance DUV LEDs is their poor hole injector due to the high dopant activation energy of Mg for $Al_xGa_{1-x}N$ with a large Al composition. P-type GaN

was used in lieu of p-type $Al_xGa_{1-x}N$ to improve the hole concentration. To tackle the challenge of poor hole injection and to further substantially enhance hole injection over p-GaN, we have recently reported the utilization of heavily p-type doped Si nanomembrane (NM) on UVC LEDs as both a contact and hole injectors.[12–14] However, the dislocations in epitaxial nitrides could form a leakage current path, which has been observed from epitaxial films of InGaN/GaN grown on single crystalline GaN substrates[15,16] and also AlGaN on sapphire substrates.[10] Understanding the influences of the dislocations on UV LED performances will help in understanding the limitations of light emission efficiency for nitride-based LEDs and pave the way for improvement of nitride materials growth and effective adaptation to Si hole injector technology.

In this work, to investigate the dislocation hillocks and their impact on light emission performances, we examined the surface morphology and defects traits of an epitaxially grown high Al-composition $Al_{0.55}Ga_{0.45}N/AlN$ multiple quantum well (MQW) structure on AlN substrate through conductive atomic force microscopy (CAFM). We performed the photoluminescence (PL) measurements on the as-grown epitaxial structure and electroluminescence (EL) measurements on the same epitaxial structure implemented with a p-type Si hole injector.[12–14] The PL and EL spectra exhibited disparity in terms of light emission output and wavelength shift. Through the CAFM study, it was found that the disparity correlates to the open-core dislocations in the epitaxial structure through both the formation of current leaky paths and composition inhomogeneity (i.e., Ga rich) at the dislocations.

The detailed layer structure of the UVC LED is illustrated in Figure 1(a). The structure was grown on an AlN substrate by low pressure organometallic vapor phase epitaxy (LP-OMVPE) in a custom-designed high-temperature reactor. The precursors for Al, Ga, N, Si, and Mg were trimethylaluminum, triethylgallium, ammonia, silane, and bis(cyclopentadienyl)-magnesium, respectively, in a

hydrogen diluent. As shown in Fig. 1(a), on a (0001) c-plane AlN substrate, a Si doped 600 nm $n-Al_{0.74}Ga_{0.26}N$ electron injection layer with a doping concentration of 8×10^{18} cm^{-3}, a 31-period 2 nm $Al_{0.55}Ga_{0.45}N$/6 nm AlN MQW, and a 100 nm Mg doped (4×10^{18} cm^{-3}) grading layer from AlN to $Al_{0.7}Ga_{0.3}N$, which was intended to increase the number of free holes due to impact ionization effects.[17] Following the grading layer, a 10 nm Mg doped (5×10^{18} cm^{-3}) p-GaN layer was grown to circumvent the oxidation of the AlN surface.[14] At present, optical pump lasing results obtained from a laser bar made of the similar epitaxy structure have been obtained.[18] Despite the optical pump results, realizing electrical pumped lasers encountered great challenges in terms of light emission power and wavelength shift.

The bulk AlN substrates that we used for the growth of LEDs have a low dislocation density of $<10^4$ cm^{-2}.[19] However, structural defects in AlGaN film can be formed during AlGaN epitaxial growth process due to various factors such as the seed volume, AlN surface, improper seed fixation penetrating the growing crystal, and accumulated stress within large number of quantum wells.[20] Under microscope examination, the hillocks were observed to be randomly located on the top surface of the finished epitaxial structure (Figure 1(b)). The visible screw dislocation density of the epitaxy material is estimated to be around $10^5 \sim 10^6$ cm^{-2} (see supplementary material for more details). Each hillock extends to an area about over hundreds of μm^2. The epitaxy sample was optically pumped at room temperature using a 193 nm UV excimer laser source with a 7 ns pulse width and 200 Hz repetition rate. The emission was collected into a fiber cable and coupled to a monochrometer to obtain the PL spectrum. The PL spectra are depicted in Figure 1(c). As the pumping power increased from 250 to 2800 KW/cm^2, the light emission from the sample exhibited a nearly linear increasing trend versus the pumping power, as shown in Figure 1(d). The peak wavelength of the spectrum was centered at 251 nm, which correlates
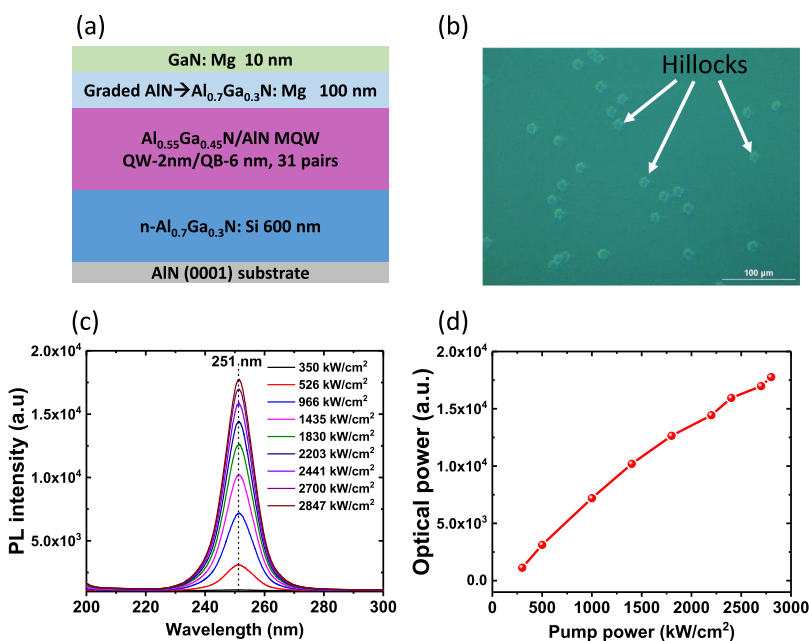
FIG. 1. (a) Schematic illustration of the epitaxial $Al_xGa_{1-x}N/AlN$ LED structure. (b) An optical microscope image taken under the differential interference contrast mode of the surface area of the epitaxial sample showing scattered hillocks. (c) Photoluminescence (PL) spectrum measured from the epitaxial structure of (a) using a 198 nm excimer laser. (d) Plot of PL optical power versus pumping power densities.

with the quantum well material composition ($Al_{0.55}Ga_{0.45}N$) in the MQW. The PL spectra verified the material integrity of the MQWs. To clarify, the PL spectrum shown in Fig. 1(c) was obtained from a nearly hillocks-free region. When the pumping light spot is illuminated on the hillocks-rich region of the epitaxy wafer, the peak intensity reduces and a side peak appears (see details in supplementary material).

To obtain the EL spectra of the sample, the epitaxial structure was fabricated into LEDs following the previously described fabrication procedures[14] to incorporate a p-type doped (5×10^{19} cm^{-3}) single-crystalline Si NM as the hole injection layer (Figures. 2(a) and 2(b)). The inset of Fig. 2(a) shows a microscope image of the sample after the Si NM was transferred to a 7 mm×7 mm size epitaxial sample. Fig. 2(b) shows a zoomed-in optical microscopic image of Fig. 2(a) under a differential interference contrast mode, where an overall conformal contact, with the exception of the dislocations area (yellow circles), between the Si NM and epitaxy sample surface was observed. The schematic of the final fabricated LED structure with electrical injection is shown in Figure 2(c), with a cathode metal stack of Cr/Ti/Al/Ti/Au in contact with the n-$Al_{0.7}Ga_{0.3}N$ and an anode metal of Cr/Au formed on the p-Si NM. The optical microscope image of fabricated LEDs can be found in previous reports.[12–14]

The current-voltage (I-V) curve in its linear scale measured from the fabricated LED is plotted in Fig. 2(d) and the inset of Fig. 2(d) shows the I-V curve in the log scale. As shown in the I-V curve, a high leakage current was observed under reverse bias. The LEDs also show a high turn-on voltage. We attribute the high turn-on voltage to the following factors: 1) the tunneling junction voltage between Si and GaN, 2) the 100 nm-thick p-grading layer from AlN to $Al_{0.7}Ga_{0.3}N$, 3) the large number of QWs pairs, and 4) the non-ohmic metal contact with n-$Al_{0.7}Ga_{0.3}N$ layer.[13]

The measured EL spectra of the LED under different current injection values are shown in Figure 2(e). The power intensity increased with increase in the forward-bias current level. The PL spectra (Fig. 1(c)) and the EL spectra (Fig. 2(e)) are plotted together in Figure 2(f) for a direct comparison. The power densities of the two sets of spectra were obtained under an identical light collecting setup to make an easy comparison. As shown in Fig. 2(f), the EL power intensity was substantially reduced in comparison to that of the PL. Of more significance, the peak wavelength of the EL spectrum shifted from 251 nm (4.939 eV) to 264 nm (4.696 eV). By comparing the PL and EL spectra, the following can be observed: 1) the primary radiative recombination regions have deviated from the expected $Al_{0.55}Ga_{0.45}N$/AlN MQWs to regions that have less Al;[21] and 2) the quantum efficiency for the radiative recombination centers under electrical injection was substantially degraded.

To trace down the origin of the disparity between the PL and EL spectra, surface morphology, compositional distribution of the as-grown epitaxial structure, and the electrical current path across the structure from the p contact to the n contact were examined using scanning electron microscopy (SEM), energy dispersive spectroscopy (EDS), and CAFM, respectively. CAFM was also performed
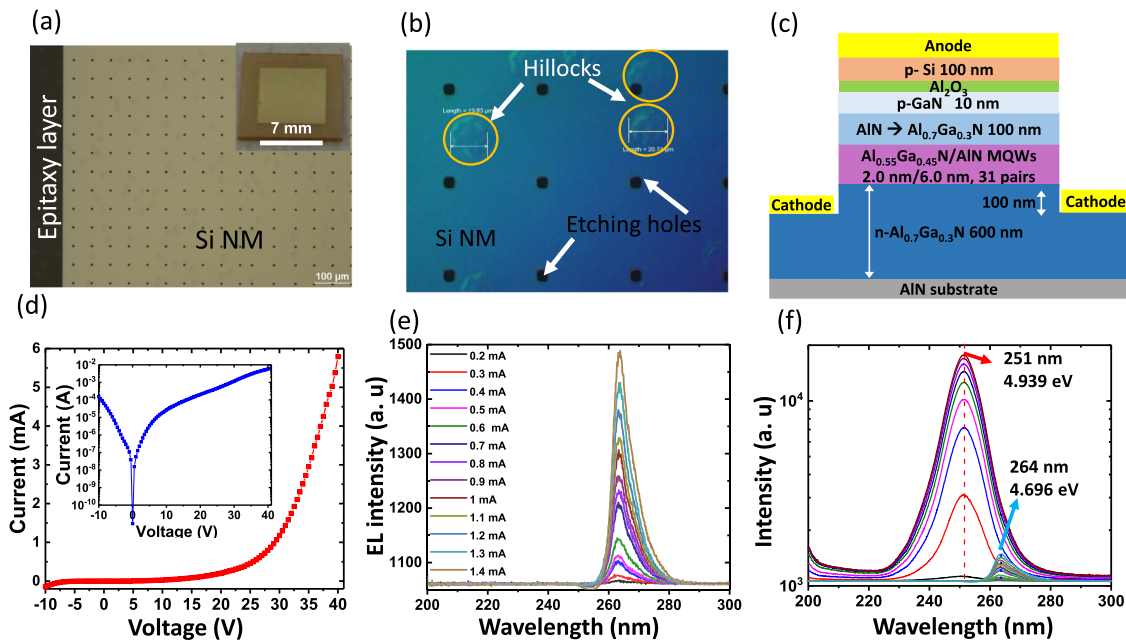
FIG. 2. Structure and characteristics of electrically injected DUV LEDs with p-type Si as contact and hole injector. (a) An optical microscope image of an $Al_xGa_{1-x}N$/AlN sample with Si NM bonded on its top. (b) A magnified optical microscope image taken under the differential interference contrast mode of (a) showing hillocks details. Black dots denote etching holes of Si NM. (c) Schematic illustration of fabricated LEDs. (d) Measured I-V curve of the LED in its linear and log scales (inset). (e) Electroluminescence (EL) spectrum obtained under different injected current levels, ranging from 0.2 mA to 1.4 mA. (f) Combined plot of Fig. 1(c) and Fig. 2(e) to show the disparity between the PL and EL spectra in terms of both wavelength and power intensity.

to examine the surface morphology as well as the influences of different types of defects on the electrical properties of the as-grown epitaxial sample.[10] The sample's top surface was scanned using a Park Systems XE-70 AFM at a rate of 0.7 Hz using a platinum (Pt) coated tip with a radius of around 25 nm in the contact-mode, and a cantilever with a nominal spring constant (k) of 0.2-N/m. To electrically connect to the conductive n-type layer, the test sample was etched down to the n-AlGaN contact layer and a Ni/Al/Ti/Au contact metal was deposited on top of the n-AlGaN layer, which later was wire-bonded to the sample mount. The CAFM tip was electrically grounded and the metal contact was kept at -5V for all scans. Equivalently, a forward 5 V bias was applied across the as-grown epitaxial structure. The scanned CAFM images are shown in Figure 3.

Two representative types of hillocks were identified, as shown in Figure 3. One type (type A) had no holes (pits) (Fig. 3(a)) and the other type (type B) had open holes (open-core dislocations) at or near the center of the hillocks (Fig. 3(c)). Figure 3(a)i (3D) and Fig. 3(a)ii (2D) show the CAFM image of the type A hillocks and Fig. 3(a)iii shows a plot of a line-scan across the center of the hillock. For these types of hillocks, no noticeable leakage current paths were

spotted in the current mapping scan as shown in Fig. 3(b)i (3D) and Fig. 3(b)ii (2D). The measured leakage current is only a few nA under -5V bias as shown in Fig. 3(b)iii.

In Fig. 3(c)i (3D) and Fig. 3(c)ii (2D), the surface morphology of type B hillocks scanned across a 20×20 μm² area shows a staircase-shaped microstructure with an open hole at the center of the highest plateau. Fig. 3(c)iii shows a line scanning across the hillock passing the center hole revealing a 300 nm deep dip. Given that the actual depth could be even greater than the measured value due to the limitation of the probe tip radius (>20 nm), the open-hole dislocation almost penetrated down to the n-AlGaN contact layer according to the layer thickness in Fig. 1(a). Fig. 3(d)i (3D) and Fig. 3(d)ii (2D) illustrate the mapping of the CAFM-tip current distribution over the same hillock region of Fig. 3(c). The brighter color indicates the higher leakage current levels that flow from the n side to the p side (reverse bias) through the epitaxial structure. The data plot (Fig. 3(d)iii) together with the line scan (Fig. 3(c)) clearly show a distinct current peak at the dip, which is about 1.6 μA, orders of magnitude higher than the current measured in the surrounding area. It is noted that the leakage current in Fig. 2(d) is also in the ~μA level under -5 V bias, which indicates that these open-hole dislocations
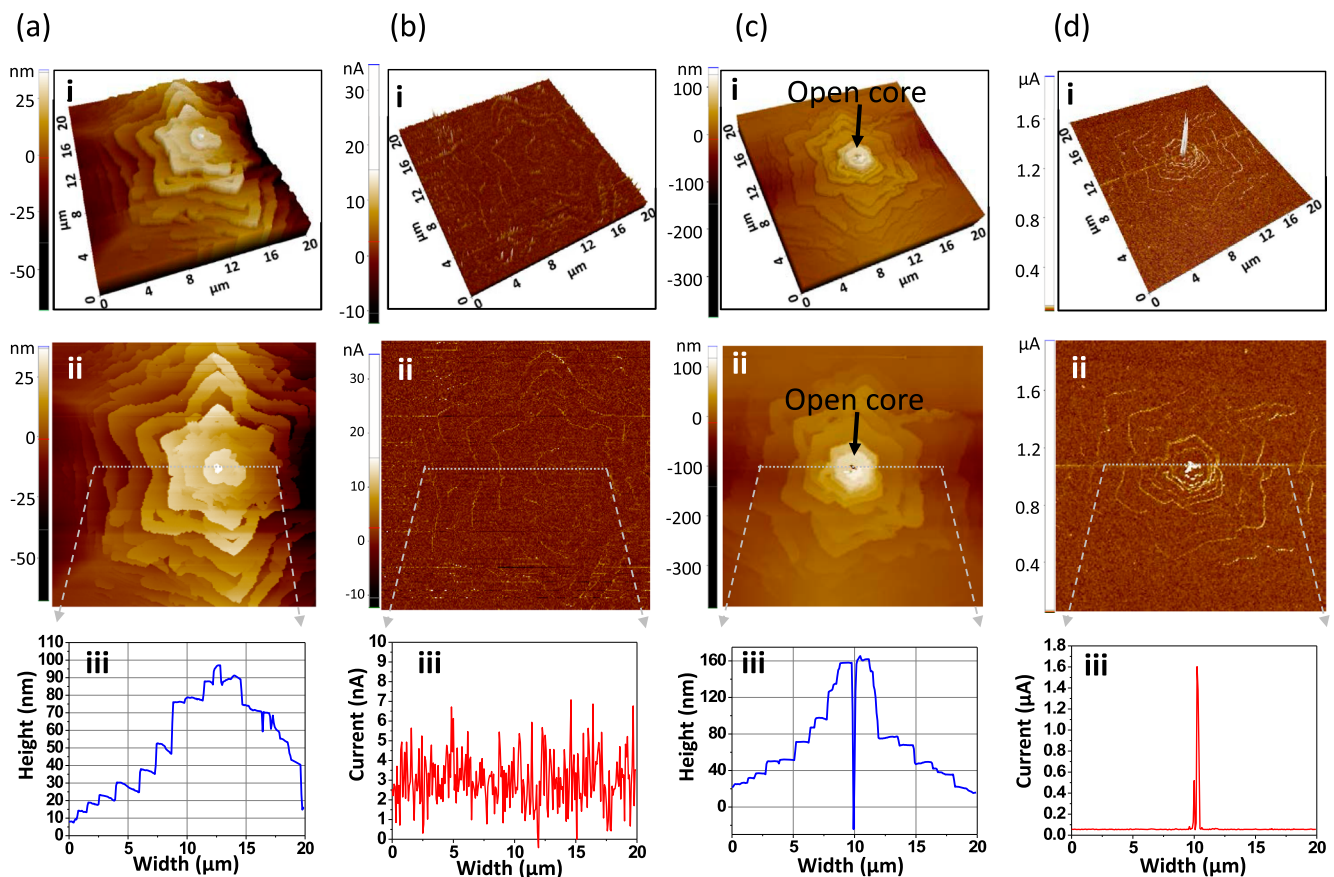
FIG. 3. Surface topography and current mapping over hillock regions characterized by CAFM measurements. (a) Topography and (b) current mapping of type A hillocks without open-core dislocations. (c) Topography and (d) current mapping of type B hillocks with open-core dislocations. In (a)-(d): i) 3D topography and current mapping, ii) 2D topography and current mapping across a hillock with flat plateau over an area of 20×20 um², and iii) line profiling along the center across the hillock terrain.

could be the predominant leakage current paths for the electrical injected LEDs when they are reverse biased.

The electrical conductive channel through the open core dislocation is speculated to originate from trap state formation due to impurity segregation[15] along the inner walls of the pits, which is similar to what was previously observed in GaN grown on c-plane sapphire substrates.[10] Consequently, the efficiency of LEDs made from such epitaxial materials was severely degraded due to the bypassing/shunting electric current inside the p-n junctions without radiative recombination in quantum wells. This explains the poor EL intensity measured from the UVC LEDs in this study (Fig 2(e) and Fig. 2(f)). In addition, it is known that the dislocation sites are always accompanied by the formation of donor- or acceptor-type states due to growth defects or Ga vacancy.[22] While these dislocation sites could also contribute to the electroluminescence (still direct bandgap), the emissions should occur at longer wavelengths since the recombination involves trap levels within the bandgap. The recombination transition could be either from a shallow donor to valence band or from a conduction band to a deep acceptor level.

Wet etching is commonly used to determine the dislocations growth conditions, as the etchant penetrates into the pits of the dislocations and makes crystal orientation-dependent etching. We used pure phosphoric acid heated to 100°C for 30 mins for our wet etching. Figure 4(a) and Figure 4(b) show the SEM images of type A and type B hillocks after the wet etching, respectively. Fig. 4(a) does not show a pit within the plateau after wet etching. In contrast, the

hillock shown in Fig. 4(b) displays a hexagonal-shaped pit within the hillock, which is attributed to the existence of an open-core threading dislocation, manifested after wet etching towards {10$\bar{1}$0} facet planes.[10,16] Corresponding to the hillocks, the element compositions of the center of the hillocks, measured by EDS, are displayed in insets of Fig. 4(a) and Fig. 4(b), respectively. As reference, the EDS measurement was also carried out on a hillocks-free area (Fig. 4(c)). By comparison, it was found that the Al component peak was significantly reduced at the center of the hillock regions for both types of hillocks. The EDS spectra confirmed that both types of hillocks are Ga-rich (less Al) compared with the non-hillock area. Thus, it was inferred that the Al composition inhomogeneity at the hillocks center could also be responsible for the EL wavelength red shift considering the current leakage paths and recombination therein with generated photons energy less than the targeted QWs region due to the reduced bandgap. To improve the performance of nitride-based DUV LEDs,[12–14] minimizing the density of open-core dislocations deems to be necessary.

In summary, we investigated close-core and open-core threading dislocations formed in an $Al_xGa_{1-x}N$/AlN MQW structure designed for electrical pumped DUV-LEDs. The open-core threading dislocations were identified to have detrimental effects on the LED performance by inducing a large leakage current and non-radiative recombination trap states. Moreover, the decreased emission photon energy under electrical injection compared to the PL emission was attributed to two factors: 1) The higher Ga
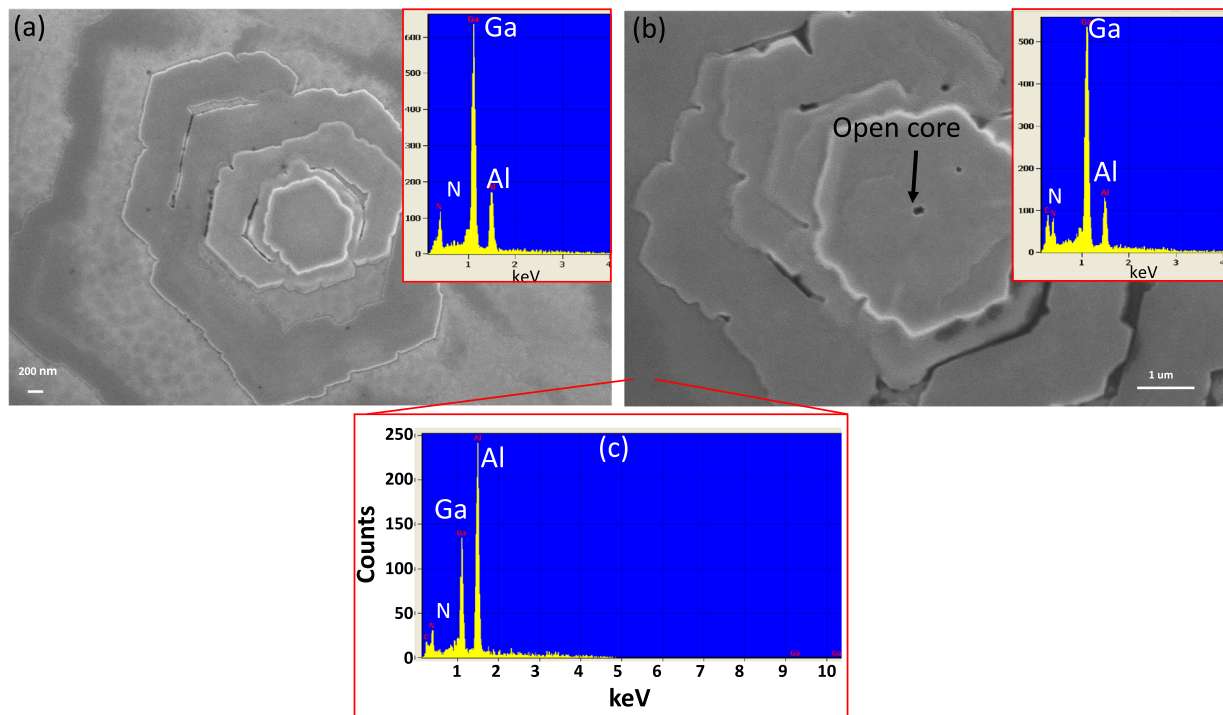
FIG. 4. An SEM image of a hillock (a) without and (b) with open-core dislocation after wet etching. Insets: Measured composition (N, Ga and Al) distribution by EDS for (a) the center area of the hillock with a flat plateau (type A) and (b) the exposed hexagonal shaped pit region (type B). (c) The element composition spectrum in the hillocks-free area for comparison.

incorporation in the hillock region reduced the bandgap, and 2) the trap states at the open-core dislocations causing an electron transition in the trap states within the bandgap. This study reveals a degradation mechanism for high Al composition-$Al_xGa_{1-x}N$ alloy-based DUV LEDs under electrical injection and points out an optimization direction for material growth towards further realization of high efficiency DUV LEDs and lasers.

See supplementary material for 1) correlation between LED leakage current and hillocks encountered by the LEDs; 2) Estimation on visible screw dislocation density of the epitaxy material; 3) PL spectrum when the pumping light spot illuminated on the hillocks-rich region of the epitaxy wafer in comparison with Fig. 1(c) obtained on a nearly hillocks-free region.

REFERENCES

[1] G. Roelkens, P. Dumon, W. Bogaerts, D. Van Thourhout, and R. Baets, "Efficient silicon-on-insulator fiber coupler fabricated using 248-nm-deep UV lithography," IEEE Photonics Technology Letters **17**, 2613–2615 (2005).

[2] P. H. Hart, S. Gorman, and J. J. Finlay-Jones, "Modulation of the immune system by UV radiation: More than just the effects of vitamin D?," Nature Reviews Immunology **11**, 584 (2011).

[3] M. Würtele et al., "Application of GaN-based ultraviolet-C light emitting diodes–UV LEDs–for water disinfection," Water Research **45**, 1481–1489 (2011).

[4] S. Abe et al., "Master recording for high-density disk using 248 nm laser beam recorder," Japanese Journal of Applied Physics **41**, 1704 (2002).

[5] H. Hirayama, N. Maeda, S. Fujikawa, S. Toyoda, and N. Kamata, "Recent progress and future prospects of AlGaN-based high-efficiency deep-ultraviolet light-emitting diodes," Japanese Journal of Applied Physics **53**, 100209 (2014).

[6] F. Mehnke, L. Sulmoni, M. Guttmann, T. Wernicke, and M. Kneissl, "Influence of light absorption on the performance characteristics of UV LEDs with emission between 239 and 217 nm," Applied Physics Express **12**, 012008 (2019).

[7] H. Amano et al., "Defect and stress control of AlGaN for fabrication of high performance UV light emitters," Physica Status Solidi (A) **201**, 2679–2685 (2004).

[8] M. Kneissl et al., "Advances in group III-nitride-based deep UV light-emitting diode technology," Semiconductor Science and Technology **26**, 014036 (2010).

[9] A. Mogilatenko et al., "V-pit to truncated pyramid transition in AlGaN-based heterostructures," Semiconductor Science and Technology **30**, 114010 (2015).

[10] M. Moseley et al., "Electrical current leakage and open-core threading dislocations in AlGaN-based deep ultraviolet light-emitting diodes," Journal of Applied Physics **116**, 053104 (2014).

[11] M. W. Moseley et al., "Detection and modeling of leakage current in AlGaN-based deep ultraviolet light-emitting diodes," Journal of Applied Physics **117**, 095301 (2015).

[12] D. Liu et al., "229 nm UV LEDs on aluminum nitride single crystal substrates using p-type silicon for increased hole injection," Applied Physics Letters **112**, 081101 (2018).

[13] D. Liu et al., "226 nm AlGaN/AlN UV LEDs using p-type Si for hole injection and UV reflection," Applied Physics Letters **113**, 011111 (2018).

[14] S. J. Cho et al., "P-type silicon as hole supplier for nitride-based UVC LEDs," New Journal of Physics **21**, 023011 (2019).

[15] B. Kim et al., "Investigation of leakage current paths in n-GaN by conductive atomic force microscopy," Applied Physics Letters **104**, 102101 (2014).

[16] S. Lee et al., "Origin of forward leakage current in GaN-based light-emitting devices," Applied Physics Letters **89**, 132117 (2006).

[17] J. Simon, V. Protasenko, C. Lian, H. Xing, and D. Jena, "Polarization-induced hole doping in wide–band-gap uniaxial semiconductor heterostructures," Science **327**, 60–64 (2010).

[18] A. R. Kalapala et al. in Gallium Nitride Materials and Devices XIV, 109180I (International Society for Optics and Photonics).

[19] HEXATECH, INC., Overview, http://www.hexatechinc.com/aln-technology-overview.html (2019).

[20] M. Kneissl and J. Rass, III-Nitride ultraviolet emitters (Springer, 2016).

[21] U. Jahn et al., "Correlation between optical and structural properties of (Al, Ga)N layers grown by MOCVD," Physica Status Solidi (A) **204**, 294–298 (2007).

[22] C. Soh et al., "Assignment of deep levels causing yellow luminescence in GaN," Journal of Applied Physics **96**, 1341–1347 (2004).